Aerosol Physics for the Lunar Environment: Equations for Lunar Dust Control and Mitigation Technologies

Nima Afshar-Mohajer¹ Gradient Corporation, Boston, Massachusetts, 02108

and

Marit E. Meyer² NASA – Glenn Research Center, Cleveland, Ohio, 44135

Sticky and jagged dust was ubiquitous during the Apollo missions, causing soiling and abrasion problems with seals, coatings and equipment, in addition to eye irritation and breathing discomfort in the cabin. The Artemis Program of NASA aims to place astronauts on the lunar surface by 2024 and establish a sustainable presence in the following decade. Returning to the Moon requires controlling and mitigating the dust which will be inevitably brought inside the cabins. The state-of-the-science for effective collection of aerosols is based on dynamics of airborne particulate matter under terrestrial conditions. However, the governing physics does not apply to extra-vehicular activity in the hard-vacuum lunar condition. For example, the substantial difference in gravity will dictate particle transport both outside and inside the cabin. In this study, we revisited the aerosol physical phenomena that are assumed in the design of Earth-based aerosol instruments and extend the applicability to different scenarios in lunar missions. As shown, long-term lunar habitats, transfer vehicles to lunar orbital platforms, and low pressure cabin atmospheres have different aerosol dynamics. In all cases, the impact of dust control strategies using gravitational, electrical, and thermal techniques for various mitigation and monitoring hardware is explored. The guidelines provided through this study will show how terrestrial aerosol equipment can translate to lunar dust applications.

Nomenclature

= terrestrial gravitational acceleration (~9.81 m/s²) g lunar gravitational acceleration (in m/s²) g_l = terrestrial acceleration of a falling particles (in m/s²) a_t lunar acceleration of a falling particle (PM) (in m/s²) a_1 terrestrial dynamic viscosity $(1.81 \times 10^{-5} \, \text{Pa.s at NTP})$ и dynamic viscosity in the lunar cabins (in Pa.s) ρ_{ld} average lunar dust particle material density (in kg/m³) air density in terrestrial conditions (in kg/m³) ρ_{ta} air density in lunar conditions (in kg/m³) ρ_{la} C_c terrestrial Cunningham slip correction factor (unitless) C_{cl} lunar Cunninghams lip correction factor (unitless) particle diameter (in µm) d_{vp} = volumetric diameter of particulate matter (PM) (in m³) = lunar electric surface potential (in V) PM particulate matter F_{h} = buoyancy force (in N)

¹ Air Quality Scientist, Environmental Sciences, Gradient Co., One Beacon Street, 17th Floor, Boston, MA 02108.

² Research Aerospace Engineer, Low-Gravity Exploration Technology Branch, NASA-Glenn Research Center, 21000 Brookpark Road, Cleveland, OH 44135

 F_g = gravitational force on the Earth (in N)

 $\vec{F_d}$ = drag force (in N)

 F_e = electrostatic force (in N)

 λ_D = Debye's sheath effective length of the electric field on the lunar surface (in m)

 F_{bl} = buoyancy force on the Moon (in N) F_{gl} = gravitational force on the Moon (in N)

 F_{dl} = drag force on the Moon (in N)

 ϵ_0 = permittivity of the lunar space (~8.85×10⁻¹² F/m)

NTP = terrestrial normal temperature and pressure (20°C and 1 atm)

PSD = particle size distribution

H = initial elevation of falling lunar dust outside Debye's length (in m)

 F_{vdw} = van der Waals force (in N) F_i = image force (in N) γ_s = surface energy (in J/m²)

E = electrostatic field of a charged particle in the lunar environment (in V/m) F_{rl} = minimum detachment force for a PM deposited on a lunar surface (in N)

= minimum detachment force for a PM deposited on a terres trial surface (in N)

 F_{el} = minimum dielectrophoretic detachment force for a particle adhered to a surface in lunar vacuum (in N)

 F_{et} = minimum dielectrophoretic detachment force for a particle adhered to a terrestrial surface (in N)

 T_1 = average air temperature inside lunar cabins (in K)

T_t = typical ambient air temperature inside spacecraft/lunar cabins (in K)

E = electric field (in V/m)

 F_{tht} = terrestrial thermal force acting on a particle (in N) F_{tht} = lunar thermal force acting on a particle (in N)

 T_p = particle surface temperature (in K)

 ΔT = temperature difference between the particle and collecting surface (in K)

 λ_t = terrestrial mean free path of air molecules (in µm)

 λ_l = mean free path of air molecules inside lunar landers/cabins (in µm)

I. Introduction

The United States space exploration vision for landing the first woman and next man on the Moon, initiated new momentum for research activities at the National Science and Space Administration (NASA) to secure human exploration across the solar system. This new round of lunar exploration, called Artemis, will eventually support sustainable return of humans to the Moon with extensive robotic exploration along with construction of a lunar base. This requires addressing multiple is sues experienced during the Apollo era of exploration. A wide range of problems are attributed to the dustiness of the lunar environment including dust levitation from natural and manmade activities and subsequently penetration of the dust into astronauts' cabins and onto their equipment (Cain et al., 2010; Gaier, 2007; Fuhs and Harris, 1992). Astronauts performing extra-vehicular activities (EVAs) will follow special protocols to limit the amount of lunar dust brought into the cabins on suits, tools and samples, but inevitably, some dust will be introduced and will be dispersed into the cabin air. Understanding the settling mechanism of particles suspended in the lunar environment, particularly inside a lunar lander, is of great interest, as minimum required dust concentrations must be achieved before going up to the lunar orbiter. Therefore, identification, control, and mitigation of dust hazards is one of the most important problems to be resolved for the Artemis mission.

When dust is suspended in air, it is considered an aerosol, whereas dust levitating in the vacuum of the lunar surface is referred to as 'lofted dust.' Every aerosol control/mitigation technique used on Earth exploits a certain characteristic transport property of airborne particulate matter, and these properties can be targeted and altered in order to control the particles in some way. Under terrestrial conditions, there are a wide range of techniques implementing gravitational-, electrodynamic-, filtration-, condensational-, centrifugal-, or thermal-based mechanisms for sampling or collection of the airborne or suspended particulate matter (PM) (Hinds, 1998; Kulkarni et al., 2011). Thus, the intention of this study is to adapt the aerosol dynamics formulas governing lunar dust control mechanisms and present the differences quantitatively with respect to terrestrial cases. The focus has been on the mechanisms appropriate for potential implementation in the lunar environment. This study, therefore, provides a guideline for scientists and

engineers planning lunar operations, in particular, methods for estimating effective application of dust particle control technologies on the Moon.

The following aerosol formulas are given to inform and assist in understanding the relative magnitude of particle velocities and forces, and shed light on the feasibility of implementing a control technology. However, they are limited to spherical particle geometry and other given assumptions, which significantly simplify actual conditions in terrestrial and lunar scenarios. Another necessary limitation of this work is that these are single-particle formulas, and for more realistic calculations, a numerical model must be undertaken to calculate transport and forces for a bulk of aerosol number concentration with a distribution of particle sizes (and a distribution of other particle properties as well). Some nomenclature discrepancies exist between different disciplines, so for clarity, this paper will use the term 'particle density' to refer to the density of the particle itself (mass per unit volume of the particle material), in kg/m³. Particle mass concentration, or aerosol mass concentration, also has units mass per unit volume, mg/m³, and refers to the total mass of all airborne particles.

II. Dust Settling under Gravity

Typically, PM refers to fine particles on the order of micrometers or less, which can have volumetric diameters, d_{vp} , small enough to be in the Stokes regime (Reynolds number < 1). Without exertion of any external forces, deposition of dust on surfaces occurs naturally due to the gravitational settling of particles. The classic equation for terminal settling velocity of a spherical particle falling due to gravity is presented in the first row of Table 1. Based on Newton's second law for terretrial conditions, acceleration of a falling particle, $m.(dv/dt)_z = \Sigma F_z$, is a function of gravitational force, F_g, buoyancy force, F_B, and drag force, F_D (Vincent, 1995; Hinds, 1998). For small particles (below 5 µm), the Cunningham correction factor, C_c is necessary to account for air slip at the particle surface, effectively increasing the settling velocity. However, with the absence of air molecules in the lunar atmosphere, drag and buoyancy forces, which resist against the gravitational force, do not exist. Instead, the solar radiation charges lunar dust and consequently generates an electrostatic field exerting an upward Coulombic force against falling particles (see Figure 1a). Stubbs et al. (2006) accounted for this electrostatic field surrounding the lunar surface and proposed an imaginary shield height over the surface wherein the electrostatic force, Fe, is equal to or smaller than the lunar gravitational force, F_{ol} . This shield height is the so-called Debye's length denoted by λ_D , is variable across the lunar surface. Within the Debye's length, strong cohesive forces and lunar gravity keep the particles on the surfaces. If lunar dust particles are lifted due to external forces (e.g., walking of an astronaut), they immediately return toward the lunar surface with an downward accelerating velocity (no terminal settling velocity).

As a result, Eq. (1) adapted to lunar surface conditions (hard vacuum) turns into Eq. (2). In other words, in lieu of F_B and F_D , an electrostatic field surrounds the Moon applying an electrostatic force of F_E on the falling particle (Afshar-Mohajer et al., 2011). One should note that the electrostatic field around the Moon is spatio-temporally variable, and when negligible, the falling particle in the lunar environment does not have a terminal velocity and accelerates until it reaches the lunar surface. Another case is inside a human lunar lander or pres surized rover or habitat, which does not possess hard vacuum but has an air pressure lower than the terrestrial atmospheric pressure, potentially as low as 8.2 to $10.2\,$ psi (0.56 to 0.69 atm that is roughly half to two-third of that on Earth). Consequently, there are different formulations for estimating the depositing terminal settling velocity inside and outside the cabins as summarized in Table 1:

Table 1. Maximum settling velocity of a single falling particle under different environments

Coverning equation for maximum settling velocity

Environment	Governing equation for maximum setting velocity				
On the Earth	$\frac{C_c \rho_p g d_p^2}{18\mu} = \frac{\rho_p g d_p^2}{18\mu} \times \left(1 + \frac{\lambda_t}{d_p} \left(2.34 + 1.05 \exp\left(-0.39 \frac{\lambda_t}{d_p}\right)\right)\right)$				
On the Moon, outside cabins, beyond the Debye's length	$\sqrt{\left(2g_l\lambda_D - \frac{24\varepsilon_0{\phi_s}^2}{\rho_{ld}{d_p}^2}\right)}$				
On the Moon, outside cabins, within the Debye's length	No terminal velocity. The velocity increases unlimited until it intercepts a surface: $\sqrt{(2g_lH)}$				
On the Moon, inside cabins	$\frac{C_{cl}\rho_p g_l d_p^2}{18\mu_l} = \frac{\rho_p g_l d_p^2}{18\mu(\frac{T_l}{T_t})^{0.74}} \times \left(1 + \frac{\lambda_l}{d_p} \left(2.34 + 1.05 \exp\left(-0.39 \frac{\lambda_l}{d_p}\right)\right)\right)$				

Environment

In the equations of Table 1, ρ_p is the particle density (mass per unit volume of the particle material that is constant, regardless of environment), λ and λ_1 are the mean free paths of molecules in the atmosphere on Earth or in the lunar cabin, λ_D denotes Debye's length or the height of the electrostatic shielding region above the lunar surface, ϕ_S denotes the electric surface potential varying spatially on the Moon, µ denotes dynamic visocosity of the air on Earth (about 1.85×10^{-5} Pa.s at NTP), C_c and C_{cl} denote Cunninghams lip correction factor (depends on particle size, e.g., 1.15 for a 1 μ m particle at NTP) on Earth and on the Moon. Permittivity of space, ϵ_0 , for hard vacuum condition on the Moon is approximately 8.85×10^{-12} F/m and the average lunar dust density, ρ_p , ranges between 2300 and 3100 kg/m³, and therefore is assumed to be 2700 kg/m³ in the present examples (Heiken et al., 1991). The lunar gravitational acceleration, g₁, is also different than that on the Earth and depends on the angle from the horizon and altitude from the surface ranging between 0.6 and 2.4 m/s² (Michael and Blackshear, 1972), which is approximately 4 to 16 times smaller than the terrestrial gravitational acceleration. Heiken et al. (1991) suggests 1.62 m/s² to be the best representative g_1 . The dynamic viscosity inside spacecraft cabins is a power function of temperature ($T^{0.74}$) and is proportional to the dynamic viscosity of the air on Earth, u. The average temperature within a spacecraft depends on cabin heat load, ventilation, and cabin heat loss (Menget al., 2012). The temperature in a lunar cabin may range from 10 to 26 °C, but on average is a bit cooler than terrestrial normal temperature of $T_t = 20$ °C. Here, we assume the average T₁ value to be 18 °C (Meng et al., 2012). The terminal settling velocity of lunar dust outside Debye's length cannot be established as falling particles can accelerate freely in the absence of electrostic shield or a drage force. Therefore, the terminal settling velocity (as seen in Table 1) is a function of the falling distance denoted by H, where the velocity keeps increasing until intercepting a surface.

Lack of a drag force on the Moon leads to significantly different equations for lunar surface conditions involving the two parameters λ_D and ϕ_s that are variable across different lunar locations and times. Stubbs *et al.* (2006) reported the most representative values of λ_D to be 8.6 m near terminator, 0.41 m near subsolar points, and 0.72 m in the intermediate regions (Figure 1b). Similarly, the most representative values of ϕ_s are estimated to be 36 V near terminator, 4.1 V near subsolar points, and 3.1 V in the intermediate regions.

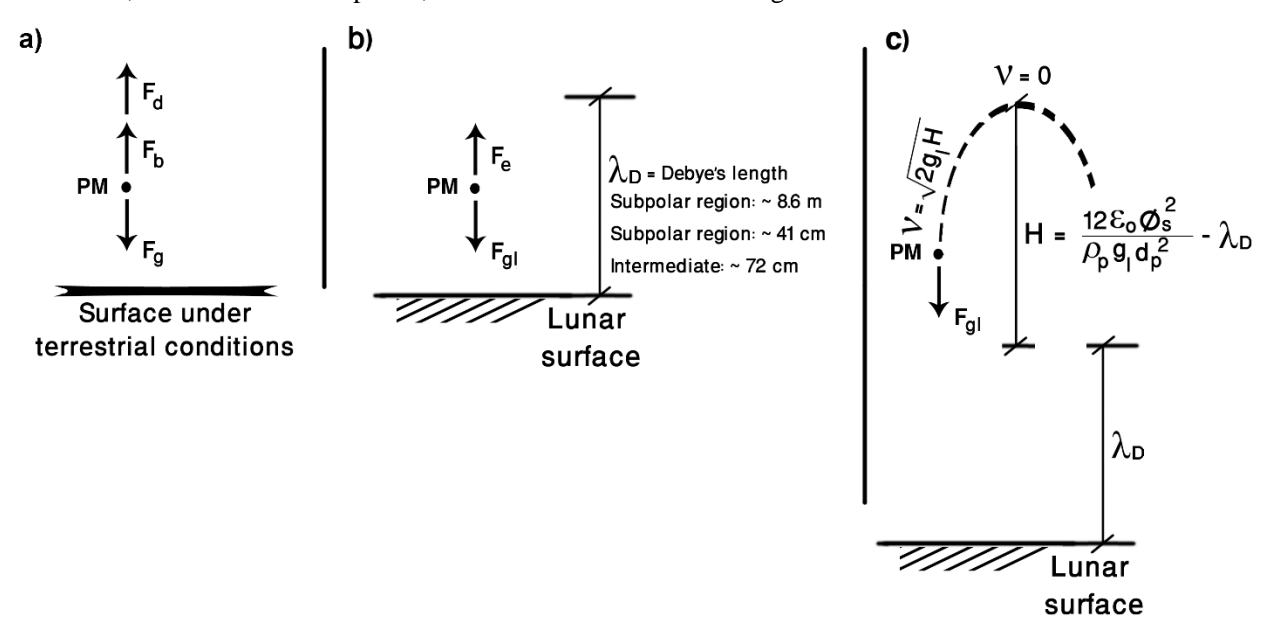


Figure 1. Free body diagrams of the forces acting on a particle under different conditions: a) terrestrial conditions, b) lunar conditions within shielding electric field of Debye's height, and c) lunar condition beyond Debye's height

The terms of the terminal settling velocity equations are depicted in the free body diagrams displayed in Figure 1, assuming a quiescent environment, which will not be the case when the astronauts are actively cleaning and moving about the cabin. However, the relative magnitudes of these settling velocities indicate that larger particles settle much faster in a pressurized environment. As mentioned before, human lunar landers are typically designed to operate at air pressures lower than Earth atmospheric pressure. The main reason for this is to reduce the number of hours necessary for prebreathing (purging the body of nitrogen to avoid decompression sickness) and achieve more extravehicular activities per mission (Abercromby et al., 2013). Another benefit from designing for reduced cabin pressure is that the vehicle must have a very heavy construction to withstand the vacuum of space, and by lowering the pressure inside

the cabin, the weight savings translates into fuel savings for the mission. For instance, the Apollo spacecraft were pressurized to only 5 psi (0.34 atm), but had a pure oxygen environment (Gatland, 1976). This lower pressure affects the settling velocity of particles inside the vehicle because it affects the drag force. Cleaning operations and various mitigation techniques will be used in the lander to reduce the amount of lunar dust in the cabin air and on the floor. Any settled particles may become airborne again on ascent into microgravity, and these will contaminate the air in the orbiting vehicle after rendezvous and hatch opening. However, once particles settle on the lander floor, they can be removed by vacuuming. Therefore, the particle size distribution (PSD) of the potential dust contamination in the orbiting vehicle can be significantly changed if sufficient time for settling elapses before ascent. Table 2 shows the settling time for different particle sizes in different conditions, falling from a height of 5.5 feet (about 1.7 m that is within the breathing zone of an astronaut). The pressures represented are terrestrial NTP 14.7 psi (101.4 kPa), 10.2 psi (70.3 kPa) and 8.2 psi (56.5 kPa) corresponding to two different potential lunar lander cabin pressures, and 5 psi corresponding to the Apollo spacecraft cabin pressure. For comparison purposes, two scenarios on Earth are included in Table 2: at sea level, and at an altitude of 30,000 feet (9144 m), where atmospheric aerosols are subject to these equations.

Table 2. Estimated settling times of a falling particle (in minutes) falling from 1.7 m above surfaces under different ambient pressure conditions (average lunar dust particle density of 2700 kg/m³ and spherical particles were assumed in all cases)

$ \begin{array}{c} d_p \\ (\mu m) \end{array} \begin{array}{c} Earth \\ (sea \\ level) \end{array} $	Farth	Earth (30,000	Pressure inside a lunar cabin			
	ft above sea level)	14.7 psi	10.2 psi	8.2 psi	5 psi	
0.02	75,475	23,814	452,255	319,043	258,356	159,356
0.5	1,044	636	6,256	5,612	5,171	4,068
1	298	223	1,789	1,683	1,606	1,393
5	13.5	12.6	80.8	79.6	78.7	76.0
10	3.4	3.3	20.5	20.4	20.3	19.9
20	0.86	0.85	5.2	5.2	5.1	5.1
100	0.11	0.11	0.66	0.66	0.66	0.66

As seen from Table 1, it is evident that the settling time inside lunar cabins is drastically more sensitive to changes in the particle size compared to the terrestrial environment. In fact, the smallest particles take much longer to settle because their motion is in the Stokes regime causing slip (reducing drag), and their relatively smaller mass, which is not affected significantly by gravity. For a certain particle size, increasing the air pressure inside cabins increases the settling time (decreases the terminal settling velocity). However, for larger particles (i.e., 10 µm and above) the settling times at different air pressures in all environments are nearly the same. A 20-um particle in a lunar cabin maintained at a pressure of 10.2 psi requires about 5 minutes to descend from the astronaut's breathing zone down to the cabin floor. This size of particle would not be eliminated entirely, as some may remain adhered to non-horizontal surfaces which may not be vacuumed in the cleaning process. The finer particles that can easily levitate from the lunar surface according to the proposed fountain model by Stubbs et al. (2006), remain suspended in the air cabin longer than the larger ones. However, gravity has more impact on particle settling than lower air pressures. For example, it takes about 5 hr for a 1-µm lunar dust particle falling from 1.7 m elevation to reach the floor on Earth, but in a lunar cabin on the Moon with the same air pressure, the settling time increases to $\sim 30 \,\mathrm{hr}$, which is roughly a factor of (g_1/g_1) times greater. The lowest cabin air pressure of 5 psi, reduces this settling time from 1,789 min (~30 hr) to 1,393 min (~23 hr). Table 1 refers to one dust particle size for each condition, but lunar dust is not monodisperse. The particle size distribution (PSD) is a more important parameter than gravity and the cabin air pressure for the control of lunar dust.

An entire particle size distribution of lunar dust particles can be addressed with these aerosol physics equations to design an HVAC system for the lunar cabin. When a group of particles with a certain PSD enters the cabin, the particles fall to the floor (or other surfaces) at different times. The PSD varies with time and the mode of the PSD shifts to smaller sizes until all particles deposit. For example, changes in the PSD of suspended dust in a lunar cabin can be calculated. This is shown in Figure 2, where the PSD of an initial dust contamination event is shown (Figure

2a), followed by two arbitrary elapsed times, 4 hr (Figure 2b) and 12 hr after setting (Figure 2c), for both lunar dust and the lunar dust simulant JSC-1Af (properties adapted from Park *et al.* (2008)).

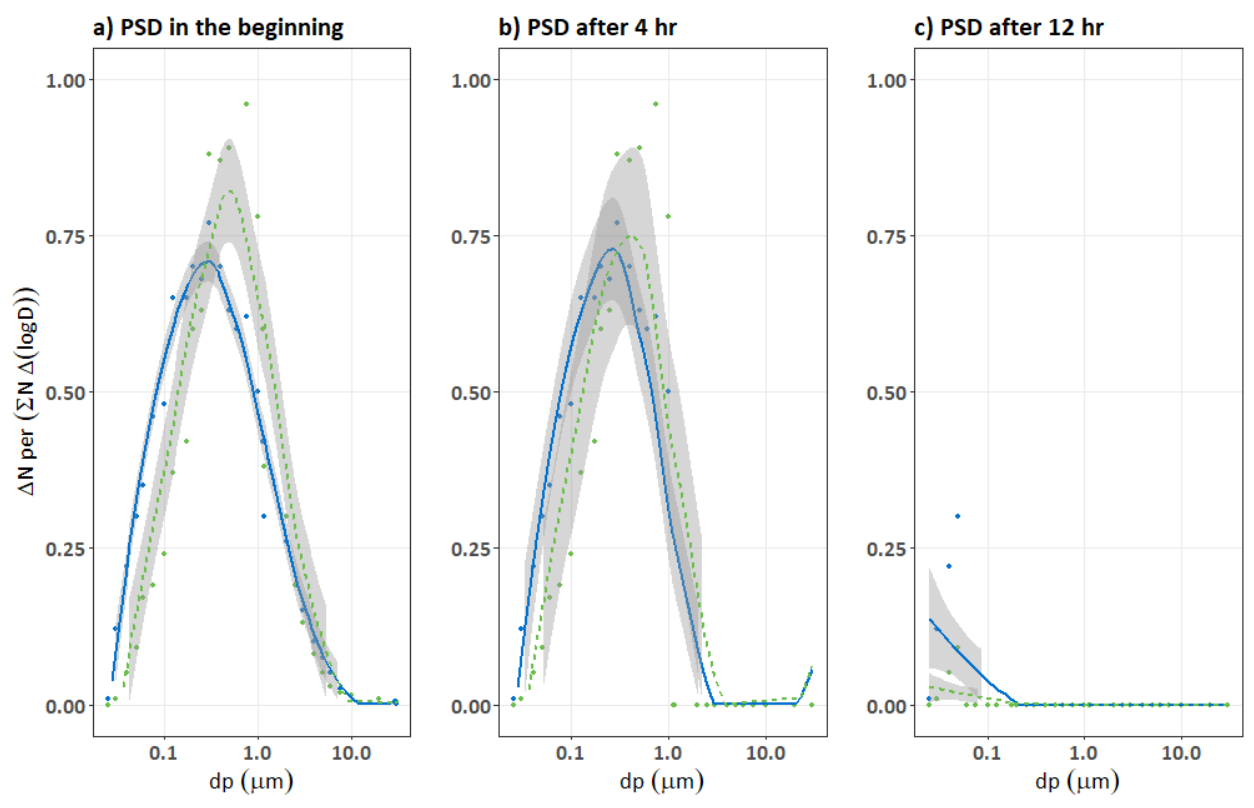


Figure 2. Changes to a particle size distribution that may occur in a lunar dust contamination event in a lunar cabin. The initial PSD is constructed from Park et al. (2008)

When the lunar dust first enters the cabin, the PSDs are shown in Figure 2a. After four hours, Figure 2b shows the PSD truncated, with nearly all particles above 2 µm removed from the air. Then in Figure 2c, after 12 hours, only particles below 200 nm remain suspended. This demonstrates effectiveness of lunar gravity in 'cleaning' the air without any active cleaning interventions, using a realistic PSD as a starting point.

III. Estimating Dust Adhesion

Particulate matter settling results in deposition, in which surface forces act to adhere particles to surfaces or to other particles. These forces include surface electric force, F_e , image force, F_i , and van der Waals, F_{vdw} (Wanka et al., 2013). Based on a study by Walton et al. (2007), the lack of adsorbed molecules (e.g., oxygen or water) in the lunar environment results in much less surface contamination, resulting in a much higher effective surface energy than the contaminated surfaces we contend with on Earth. All particles adhered to a surface are subject to F_{vdw} , however, F_i and F_e only apply to charged particles (which is the typical state of those in the lunar environment). For the case of terrestrial PM, F_b and F_d are no longer acting on the deposited PM, but for the case of lunar dust, the surface forces of F_{vdw} , F_e , and F_i should be added to the list of forces accounted for in the velocities in Table 1. The external force required to remove a deposited particle in terrestrial vs. lunar environments are presented in Eq. (1) and Eq. (2), assuming spherical uncharged particles on Earth:

Terrestrial conditions:
$$F_{rt} = F_g + F_{vdw} = \left(\frac{\pi \rho_p g d_p^3}{6}\right) + 2\pi d_p \gamma_s$$
 (1)

$$Lunar\ conditions: F_{rl} = F_g + F_{vdw} + F_i + F_e = \left(\frac{\pi \rho_{ld} g_l d_p^3}{6}\right) + 2\pi d_p \gamma_s + \left(\pi \varepsilon_0 \phi_s^2\right) + \left(2\pi \varepsilon_0 \phi_s E d_p\right) \tag{2}$$

where γ_s is the surface energy between the tangent surfaces (0.02 to 2 J/m²) that depends on the dust particle itself and the surface materials in contact with the particle. There will be a distribution of adhesive forces, not only for a given size distribution of particles, but also because γ_s will vary for different particle morphologies, as a particle can potentially have multiple contact points given the jagged nature of lunar dust. Changes in particle surface energies in a vacuumcan be tested by soil mechanics tests of cohesive strength. Cohesion measurements of a lunar soil sample obtained from Apollo 11 were made (sealed under N_2) under vacuum of 5×10^{-9} torr. The sample was then exposed to O_2 and $O_2+3.5\%$ H_2O at different air pressures and temperatures to simulate Earth conditions. Results showed a reduction of the cohesion force after exposure to the gases in all pressure and temperature combinations (Walton, 2007). It is not practical to calculate adhesion forces for a typical lunar dust surface contamination scenario, considering an entire particle size distribution, a variety of particle morphologies and contact area geometries for each particle, not to mention agglomerates of lunar dust. But the above formulas show that the gravitational force is much smaller than the van der Waals force, given that it is proportional to the particle diameter cubed. Given the most representative average value of ϕ_s (lunar electric surface potential) of 3.1V, the image force presents a much larger adhesive force than the surface electric force.

IV. Dust Surface Detachment Using Electrostatic Fields

Electrodynamic-based technologies are among the most common control strategies in terrestrial dusty environments. The main advantages of using electrostatic/electrodynamic forces in controlling PM in industrial applications have been proven: low maintenance cost, absence of moving parts, and high efficiency compared to other methods (Parker, 1997). In contrast to terrestrial PM, lunar dust carries substantial electric charges naturally accumulated on the particles due to the exposure to cosmic rays and solar radiation (Horányi, 1996). The build-up of natural charges on lunar particles encourages the use of electrostatic-based devices to control (*i.e.*, repel, collect, or slow down) unwanted dust (Afshar-Mohajer et al., 2012 & 2014). The best application of electrostatic fields in collection of lunar dust has been practiced outside landers on the lunar surface. Sims et al. (2004), Calle et al. (2009) and Mazumder et al. (2007) proposed an effective device, an electrodynamic dust shield (EDS), for removing lunar dust deposited on solar panel surfaces. The minimum dielectrophoretic force required to remove particles adhered to surfaces in the lunar environment, Fel, is given in Eq. (3).

Lunar conditions:
$$F_{el} = \frac{\pi}{4} d_p^3 \varepsilon_1 \frac{\varepsilon_2 - \varepsilon_1}{\varepsilon_2 + \varepsilon_1} \nabla |E|^2 + F_{rl}$$
 (3)

where |E| is the absolute value of the electric field at the contaminated surface and ε_1 and ε_2 are dielectric constants of the surface and the lunar dust particle, respectively. Note that the multi-termadhesion force, F_{rl} is given in Eq. (2) and particles are assumed to be spheres. Mazumder et al. (2007) followed Eq. (3) and designed an EDS with electrode spacing of 1.27 mm, electrode width of 0.127 mm, and frequency of 4 Hz under high vacuum on a surface covered by a known surface area coverage of lunar dust simulant. Their experiments with applied voltages of 0.75, 1, 1.25 kV demonstrated >85% of surface cleaning efficiency. In terrestrial applications, this minimum dielectrophoretic force, requires replacement of the adhesion force term in the equation above with F_{rt} (see Eq. (1)).

$$\begin{split} Terrestrial\ conditions: &F_{et} = \frac{\pi}{4} d_p^{\ 3} \varepsilon_1 \frac{\varepsilon_2 - \varepsilon_1}{\varepsilon_2 + \varepsilon_1} \nabla |E|^2 \mp F_{rt} \\ &= \frac{\pi}{4} d_p^{\ 3} \varepsilon_1 \frac{\varepsilon_2 - \varepsilon_1}{\varepsilon_2 + \varepsilon_1} \nabla |E|^2 \mp \left(\frac{\pi \rho_p g d_p^{\ 3}}{6} \right) \mp 2\pi d_p \gamma_s \end{split} \tag{4}$$

Results of experimental and theroretical studies led independently by multiple groups of scientists (for example, Guo et al., 2018; Horenstein et al., 2013; Kawamoto et al., 2019) indicate that although the EDS is indeed effective in cleaning the dust from Earth-based solar panel surfaces, it requires about 3 times longer to accomplish the cleaning for the same number concentration and size distribution of the PM, which is due to the weaker electrodynamic field, E, that can be established in a terrestrial condition at a certain applied voltage (Kawamoto et al., 2011). Figure 3 compares the removal of dust from a surface (e.g., a solar panel) at different times using a 3-phase EDS, in both lunar and terrestrial conditions. Results of a two-dimensional Monte Carlo numerical simulation for a linear layer of particulate matter deposited on a horizontal surface (with assumed surface area coverage of 10%) depict the evolution of particle detachment and the significant advantage in cleaning surfaces covered in charged particles under the lunar

condition (Figure 3a) compared to terrestrial cases (Figure 3b). Trajectories of the airborne particles being lifted up and carried away from the surface reveal that the PM removal occurs faster under lunar conditions than in terrestrial conditions. The 3-phase electric field had the advantage of alternating current electric power generation, transmission, and distribution. Note that in terrestrial conditions, the smallest particles can be lifted and then transported because on Earth, particles will not be as highly charged, and thus will have weaker adhesion forces versus lunar dust particles (Kemmerer et al., 2019).

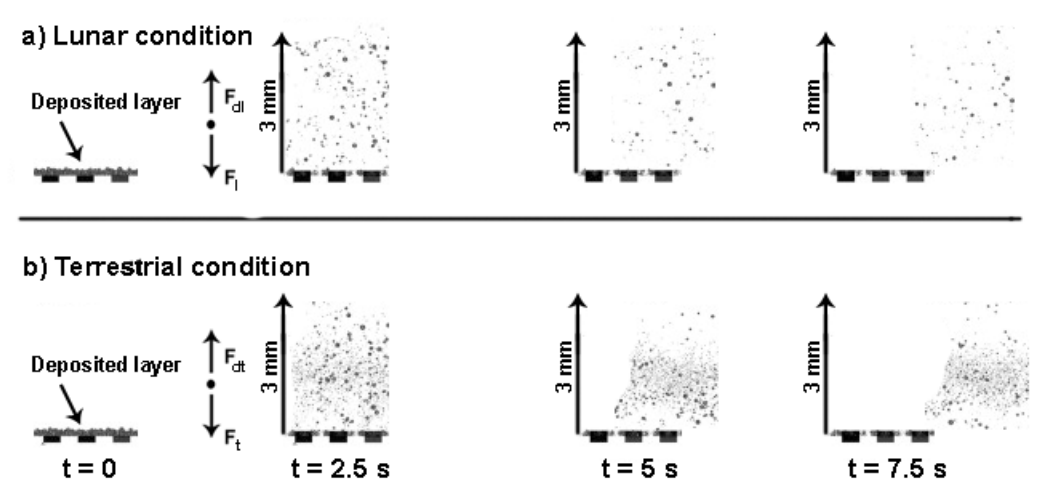


Figure 3. Removal of a deposited PM in different environments: a) under lunar condition and b) under terrestrial condition

V. Dust Control Using A Thermal Gradient

Similar to electrodynamic methods, establishing a thermal gradient is another way to control dust particles in a pressurized habitat. In the presence of a large temperature gradient, suspended particles will move in the direction of a colder region. This phenomenon, which is known as thermophoresis, can attract airborne particles to a 'cold trap' which could be a collection surface engineered at significantly lower temperatures than the surrounding air. While this will likely require a great deal of energy, there may be applications in the cabin environment for this technique, particularly for sub-micrometer particles. The thermophoretic force is a function of air density, temperature gradient, and particle size. Hinds (1998) presents an equation for the thermophoretic force, F_{tht} in Eq. (5), which is extended to lunar conditions in Eq. (6).

$$Terrestrial\ conditions: F_{tht} = \frac{-9\pi d_p \mu^2 \Delta T}{2\rho_a T_p} \times \left(\frac{1}{1+6\frac{\lambda_t}{d_p}}\right) \times \left(\frac{\frac{k_a}{k_p} + 4.4\frac{\lambda_t}{d_p}}{1+2\frac{k_a}{k_p} + 8.8\frac{\lambda_t}{d_p}}\right)$$
 (5)
$$inside\ lunar\ landers/cabins: F_{thl} = \frac{-9\pi d_p \mu_l^2 \Delta T}{2\rho_a T_p} \times \left(\frac{1}{1+6\frac{\lambda_l}{d_p}}\right) \times \left(\frac{\frac{k_a}{k_p} + 4.4\frac{\lambda_l}{d_p}}{1+2\frac{k_a}{k_p} + 8.8\frac{\lambda_l}{d_p}}\right)$$
 (6)

inside lunar landers/cabins:
$$F_{thl} = \frac{-9\pi d_p \mu_l^2 \Delta T}{2\rho_a T_p} \times \left(\frac{1}{1+6\frac{\lambda_l}{d_p}}\right) \times \left(\frac{\frac{k_a}{k_p} + 4.4\frac{\lambda_l}{d_p}}{1+2\frac{k_a}{k_p} + 8.8\frac{\lambda_l}{d_p}}\right)$$
 (6)

where constants k_a and k_p are thermal conductivity of the air and the particle material, λ_t and λ_l are mean free path of the air molecules at terrestrial and lunar conditions, respectively (which are a function of the ambient air pressure), and T_p is the average temperature on the particle surface. One should note that these equations are compared without considering other acting forces such as electrostatic forces that exist on the Moon or drag forces that exist on the Earth and in the pressurized cabin.

The most common use of thermophoresis for particle control in aeros of applications is the thermal precipitator, or thermophoretic sampler. These devices are typically designed for sampling particles for subsequent analytical techniques, such as microscopy. The use of a large thermal gradient to deposit particles onto a microscopy substrate has been used in many research efforts in the realm of atmospheric aerosols, urban pollution, indoor air quality and

smoke particle characterization, among others (Meyer, 2015). Devices have been designed to collect particles ranging from less than 10 nm to 1 µm in diameter. A thermal gradient can be increased by making the gap between the two thermal surfaces smaller, with values ranging from 0.1 mm to 1.25 mm (Azong-Wara et al., 2009, Maynard 1995, Meyer, 2015, Leith et al., 2014, Tsai et al., 1995, Wen and Wexler, 2007). Oh et al. (2020) explored the effects of thermophoresis on dust collection on terrestrial solar panels and concluded that accumulation of submicrometer particles can be reduced by incorporating a thermal gradient between the solar panel surface and ambient air temperature (Lorenzo *et al.*, 2007).

VI. Conclusions

Comparing particle behavior on Earth with different environments in lunar missions shows that there are significant differences in the aerosol physics, which can shed light on potential mitigation techniques. While on Earth, gravitational settling cleans our air of larger particle sizes, the lunar cabin only benefits from a gravitational field that is about 6 times weaker, and the drag force on airborne particles depends on the cabin pressure. Ultimately, any settled particles can be eliminated by vacuuming the floor and thus remove a significant portion of the contaminant PSD that would become airborne upon ascent to the lunar orbiter. This will limit the cross-vehicle contamination that will inevitably take place. Dust adhesion is an important mechanism to account for, as it will retain lunar dust on expensive and sensitive surfaces. These adhered particles may be re-entrained into the cabin environment unless they are cleaned by wiping. Dust mitigation by electrostatic fields is an important technique for outside habitable spaces with numerous successful prototypes demonstrated. Thermal gradients also affect particle motion, and although it may be more difficult to incorporate this into spacecraft cleaning and mitigation operations, it is a more effective technique for submicrometer sized particles. While the given aerosol formulas are subject to many simplifying assumptions and conditions, they are useful for considering order-of-magnitude comparisons of particle transport and deposition characteristics. Single-particle formulas assuming particle sphericity can be applied in numerical models to account for particle size distributions and larger concentrations. Ultimately, this work shows that changes in aerosol physics of dust in the lunar environment cannot be captured simply by replacing Earth gravity with lunar gravity terms in the governing equations.

References

Abercromby, A.F., Gernhardt, M.L., Conkin, J., "Fifteen-minute Extravehicular Activity Prebreathe Protocol Using NASA's Exploration Atmosphere (8.2 psia/34%O2)," 43rd International Conference on Environmental Systems, ICES-AIAA, Vail, CO, USA, 2013.

Afshar-Mohajer, N., Wu, C.-Y., and Sorloaica-Hickman, N., "Efficiency determination of an electrostatic lunar dust collector by discrete element method," *Journal of Applied Physics*, Vol. 112, No. 2, 2012, pp. 21, 31.

Afshar-Mohajer, N., Damit, B., Wu, C.-Y. and Sorloaica-Hickman, N., "Efficiency evaluation of an electrostatic lunar dust collector;" 41st International Conference on Environmental Systems, ICES-AIAA, Portland, OR, USA, 2011, (p. 5201).

Afshar-Mohajer, N., Wu, C.-Y., Moore, R. and Sorloaica-Hickman, N., "Design of an electrostatic lunar dust repeller for mitigating dust deposition and evaluation of its removal efficiency," *Journal of Aerosol Science*, Vol. 69, 2014, pp. 21, 31.

Azong-Wara, N., et al.: Optimisation of a Thermophoretic Personal Sampler for Nanoparticle Exposure Studies. *J. Nanoparticle Res.*, vol. 11, 2009, pp. 1611–1624.

Cain, J. R., "Lunar dust: the hazard and astronaut exposure risks." *Earth, Moon, and Planets*, Vol. 107, No. 1, 2010, pp. 107, 125. Calle, C. I., Buhler, C. R., McFall, J. L. and Snyder, S. J., "Particle removal by electrostatic and dielectrophoretic forces for dust control during lunar exploration missions," *Journal of Electrostatics*, Vol. 67, No. 2-3, 2009, pp. 89, 92.

Fuhs, S. and Harris, J., "Dust protection for environmental control and life support systems in the lunar environment," NASA N93-27979.

 $Gaier,\ J.\ R.,\ "The\ effects\ of\ lunar\ dust\ on\ EVA\ systems\ during\ the\ Apollo\ missions," NASA\ TM-2005-213610/Rev1.$

Gatland, K. W., Manned Spacecraft. 2nd Ed., Macmillan, London, UK, 1976.

Guo, B., Javed, W., Pett, C., Wu, C.-Y., Scheffe, J. R., "Electrodynamic dust shield performance under simulated operating conditions for solar energy applications," *Solar Energy Materials and Solar Cells*, Vol. 185, 2018, pp. 80, 85.

Heiken, G. H., Vaniman, D. T. and French, B. M., Lunar sourcebook-A user's guide to the Moon. Cambridge, England, Cambridge University Press, 1991.

Hinds, W. C., Aerosol Technology: Propertie, Behavior, and Measurement of Airborne Particles, 2nd ed., Wiley & Soncs Inc., Hoboken, NJ, USA, 1998, Chaps. 2, 3, 6, 8, 9, 15.

Horányi, M., "Charged dust dynamics in the solar system," Annual Review of Astronomy and Astrophysics, Vol. 34, No. 1, 1996, pp. 383, 418.

Horenstein, M. N., Mazumder, M., Sumner, R. C., "Predicting particle trajectories on an electrodynamic screen-theory and experiment," *Journal of Electrostatics*, Vol. 71, No. 3, 2013, pp. 185, 188.

Kawamoto, H., "Electrostatic cleaning equipment for dust removal from soiled solar panels," *Journal of Electrostatics*, Vol. 98, 2019, pp. 11, 16.

Kawamoto, H., Uchiyama, M., Cooper, B. L., McKay, D. S., "Mitigation of lunar dust on solar panels and optical elements utilizing electrostatic traveling-wave," *Journal of Electrostatics*, Vol. 69, No. 4, 2011, pp. 370, 379.

Kemmerer, B.W., Lane, J.E., Wang, J.J., Phillips III, J.R., Johansen, M.R., Buhler, C.R. and Calle, C.I., 2019. Electrostatic precipitator dust density measurements in a Mars-like atmosphere. *Particulate Science and Technology*, pp.1-14.

Kulkarni, P., Baron, P. A. and Willeke, K. *Aerosol measurement: principles, techniques, and applications*, 3rd ed., Wiley & Sons Inc., Hoboken, NJ, USA, 2011, Chaps. 8, 19.

Leith, D., Miller-Lionberg, D., Casuccio, G., Lersch, T., Lentz, H., Marchese, A. and Volckens, J., 2014. Development of a transfer function for a personal, thermophoretic nanoparticle sampler. *Aerosol Science and Technology*, 48(1), pp.81-89.

Lorenzo, R., et al.: "A Thermophoretic Precipitator for the Representative Collection of Atmospheric Ultrafine Particles for Microscopic Analysis." *Aerosol Science and Technology*, vol. 41, no. 10, 2007, pp. 934–943.

Maynard, A.D.: "The Development of a New Thermophoretic Precipitator for Scanning-Transmission Electron-Microscope Analysis of Ultrafine Aerosol-Particles." *Aerosol Science and Technology*, vol. 23, 1995, pp. 521–533.

Mazumder, M. K., Sharma, R., Biris, A. S., Zhang, J., Calle, C., Zahn, M., "Self-cleaning transparent dust shields for protecting solar panels and other devices," *Particulate Science and Technology*, Vol. 25, No. 1, 2007, pp. 5, 20.

Meng, F., Man, G., and Cao, J., "A simplified manned spacecraft cabin air temperature control model and its verification," 42nd International Conference on Environmental Systems, ICES-AIAA, San Diego, CA, USA, 2012, (p. 3563).

Meyer, M. E. (2015). Design of a Thermal Precipitator for the Characterization of Smoke Particles from Common Spacecraft Materials, NASA/TM—2015-218746.

Michael, W. H. and Blackshear, W. T., "Recent results on the mass, gravitational field and moments of inertia of the Moon," *The Moon*, Vol. 3, No. 4, 1972, pp. 388, 402.

Oh, Sangchul, Benjamin W. Figgis, and Sergey Rashkeev. "Effects of thermophoresis on dust accumulation on solar panels." *Solar Energy* 211 (2020): 412-417.

Park, J., Liu, Y., Kihm, K. D., Taylor, L. A.: "Characterization of lunar dust for toxicological studies. I: particle size distribution," *Journal of Aerospace Engineering*, vol. 21, no. 4, pp. 266-271.

Parker, K. R., Why an electrostatic precipitator?, Applied Electrostatic Precipitation, Springer, Dordrecht, 1997, pp. 1, 10.

Sims, R. A., Biris, A. S., Wilson, J. D., Yurteri, C. U., Mazumder, M. K., Calle, C. I., and Buhler, C. R. "Development of a transparent self-cleaning dust shield for solar panels," *ESA-IEEE joint meeting on electrostatics*, ESA-IEEE, Vol. 814, Rochester, NY, USA, 2004, (p. 3563).

Stubbs, T. J., Vondrak, R. R. and Farrell, W. M., "A dynamic fountain model for lunar dust," *Advances in Space Research*, Vol. 37, No. 1, 2006, pp. 59, 66.

Tsai, C.J.; and Lu, H.C.: Design and Evaluation of a Plate-To-Plate Thermophoretic Precipitator. *Aerosol Science and Technology*, vol. 22, 1995, pp. 172–180.

Vincent, J. H., Aerosol science for industrial hygienists. 1st ed., Elsevier, Oxford, UK, 1995, Chap. 4.

Walton, O. R., "Adhesion of Lunar Dust," NASA CR-2007-214685, 2007.

Wanka, S., Kappl, M., Wolkenhauer, M. and Butt, H. J., "Measuring adhesion forces in powder collectives by inertial detachment," *Langmuir*, Vol. 29, No. 52, 2013, pp. 16075, 16083.

Wen, J.; and Wexler, A.S.: "Thermophoretic Sampler and Its Application in Ultrafine Particle Collection." *Aerosol Science and Technology*, vol. 41, no. 6, 2007, pp. 62, 629.